Covalently Bound pH-Indicator Dyes at Selected Extracellular or Cytoplasmic Sites in Bacteriorhodopsin. 2. Rotational Orientation of Helices D and E and Kinetic Correlation between M Formation and Proton Release in Bacteriorhodopsin Micelles†

Ulrike Alexiev,‡ Thomas Marti,§,|| Maarten P. Heyn,*,‡ H. Gobind Khorana,§ and Peter Scherrer*,‡,#

Biophysics Group, Department of Physics, Freie Universität Berlin, Arnimallee 14, D-14195 Berlin, Germany, and Departments of Biology and Chemistry, Massachusetts Institute of Technology, Cambridge, Massachusetts 02139

Received May 6, 1994; Revised Manuscript Received August 25, 1994⊗

ABSTRACT: The kinetics of the light-induced proton release in bacteriorhodopsin/lipid/detergent micelles was monitored with the optical pH-indicator fluorescein bound covalently to positions 127−134 (helices D and E and the DE loop) on the extracellular side of the protein (the proton release side). Single cysteine residues were introduced in these positions by site-directed mutagenesis, and fluorescein was attached to the sulfhydryl group by reaction with (iodoacetamido)fluorescein. Two characteristic proton release times (approximately 20 and 70 μs) were observed. The faster time constant was recorded when fluorescein was attached to positions 127, 130, 131, 132, and 134, while the slower time was observed with the indicator bound to positions 128, 129, and 133. The results are rationalized by assuming specific helical wheel orientations for helics D and E and by making a choice for the residues in the DE loop: (i) The fast time constants occur with fluorescein either attached to residues 130, 131, and 132 that form the DE loop or when pointing toward the interior of the protein with its aqueous proton channel [residues 127 (helix D) and 134 (helix E)]. (ii) The slower time constants are detected with fluorescein exposed to the exterior lipid/detergent phase when bound to residues 128, 129 (both helix D), and 133 (helix E). This interpretation is supported by measurements of the polarity of the label environment which indicate for fluorescein in group i a more hydrophilic environment and for group ii a more hydrophobic environment. The fastest proton release time (10 μs) was observed with fluorescein bound to position 127. This release time equals the rise time of the main component in the formation of the M intermediate. For positions 130, 131, 132, and 134, there is an apparent delay of at least 10 μs between these two processes. The activation energy of the fast proton release time for position 130 on the extracellular side (52 ± 5 kJ/mol) is similar to that of the slowest component in the rise of the M intermediate (65 ± 5 kJ/mol). These results suggest that the formation of M and the proton release are kinetically coupled.

Bacteriorhodopsin (bR),[1] the only protein in the purple membrane of *Halobacterium salinarium*, contains a retinylidene chromophore and acts as a light-driven proton pump [Oesterhelt & Stoeckenius, 1973; for a review, see Stoeckenius and Bogomolni (1982), Mathies et al. (1991), and Ebrey (1993)]. The electrochemical gradient generated across the membrane can be used by the cell for ATP synthesis (Racker & Stoeckenius, 1974) and other energy-requiring cellular processes. Upon illumination, the chromophore undergoes a cyclic photoreaction with an *all-trans* to 13-*cis* isomerization of the retinal and the translocation of a proton from the cytoplasmic to the extracellular side of the membrane (Lozier et al., 1976). Two amino acids involved in the proton translocation have been identified by site-directed mutagenesis, Asp-85 as the acceptor of the proton from the Schiff base (Braiman et al., 1988) and Asp-96 as the proton donor to the Schiff base (Tittor et al., 1989; Otto et al., 1989). In the L to M transition, a proton is transferred from the Schiff base to Asp-85, which remains protonated for several milliseconds until the decay of O (Bousché et al., 1992). Proton release on the other hand is already detected by pH-indicator dyes in the bulk phase several hundred microseconds after the initiation of the photocycle. Thus, the proton appearing in the bulk phase is not the same proton that originated at the Schiff base in a single flash experiment, and it must have been released by

† This work was supported by grants from the Deutsche Forschungsgemeinschaft (Sfb 312-B1) and from the BMFT (03-HE3FUB) to M.P.H. and by a grant (GM 28289) from the National Institutes of Health to H.G.K.

* Correspondence could be addressed to either author.

‡ Freie Universität Berlin.

§ Massachusetts Institute of Technology.

|| Present address: Bernhard Nocht Institute for Tropical Medicine, D-20359 Hamburg, Germany.

Present address: Liposome Research Group, Department of Biochemistry, University of British Columbia, 2146 Health Sciences Mall, Vancouver, BC V6T 1Z3, Canada.

⊗ Abstract published in *Advance ACS Abstracts,* October 15, 1994.

[1] Abbreviations: bR, bacteriorhodopsin; bO, bacterioopsin; ebR, wild-type bR expressed in *Escherichia coli*; DMPC, 1,2-dimyristoyl-*sn*-glycero-3-phosphatidylcholine; CHAPS, 3-[(3-cholamidopropyl)-dimethylammonio]-1-propanesulfonate; MOPS, 4-morpholinepropanesulfonate; Tris, tris(hydroxymethyl)aminomethane; DMF, dimethylformamide; EDTA, ethylenediaminetetraacetic acid; DTT, 1,4-dithio-DL-threitol; SDS, sodium dodecyl sulfate; IAF, 5-(iodoactamido)-fluorescein; CAF, fluorescein bound to cysteine (cysteine−(thioacetamido)fluorescein); AF, fluorescein bound to cysteine in bacteriorhodopsin; pK_{app}, apparent pK, the pK determined at the given ionic strength. The mutants are characterized by the replaced amino acids as follows: the letter before the number indicates the original amino acid in that position while the letter following the number represents the substituting amino acid using single letter code (e.g., V130C: valine in position 130 is replaced by cysteine).

0006-2960/94/0433-13693$04.50/0

some unknown group XH. At least one other group or residue must be involved in the proton release pathway between Asp-85 and the extracellular surface. For example, it has been suggested that Arg-82 and water may participate (Braiman et al., 1988; Otto et al., 1990). These ideas are in accordance with the structural model of Henderson et al. (1990), in which the distance between Asp-85 and the extracellular surface is too large for a single proton transfer step. This model also suggests the existence of a large aqueous pore or channel between the counterion to the Schiff base and the extracellular surface of the membrane. The group XH may or may not release the proton to the extracellular side in a concerted manner with the protonation of Asp-85. One goal of this study is to investigate if a kinetic coupling exists between these two processes. This is still an open question. For example, evidence was recently presented that proton release does not occur during the L to M transition (protonation of Asp-85) but rather between two distinct M substates (Zimanyi et al., 1992). This implies the absence of coupling.

To establish a possible correlation between the proton release kinetics detected with pH-indicators and the kinetics of the photocycle intermediates, it is necessary to show that the detection time of the proton by the indicator is not limited by diffusion on and from the surface to the dye. In the preceding paper (Scherrer et al., 1994), we showed that the proton release times detected with fluorescein bound to either the extracellular (22 μs) or cytoplasmic (61 μs) loops were shorter than those detected with the bulk indicator pyranine (125 μs). A dye bound to the extracellular surface is thus required for a proper time resolution of proton release. Moreover, the protons released appear to be retained at the surface and to migrate rapidly along the micellular surface to the cytoplasmic side. In this work, we bound the pH-sensitive dye fluorescein to different positions in the helices D and E and in the DE loop (positions 127−134) and measured the proton release kinetics on the extracellular surface.

This study shows that the proton release times detected on the extracellular surface vary with the attachment site for the pH-indicator and fall into two groups. For the first group of sites, a fast release time was observed with the label in a hydrophilic environment. For the second group, the release times were about 3-fold slower, and the label was in a more hydrophobic environment. These results define the helical wheel orientation of the helices D and E and the residues in the loop between them. In addition, we found that the kinetics of proton release are concurrent with the second and main component in the rise of M with the label attached at 127, whereas in all other positions it is delayed with respect to this component by at least 10 μs.

MATERIALS AND METHODS

Chemicals. 3-[(3-Cholamidopropyl)dimethylammonio]-1-propanesulfonate (CHAPS); 1,2-dimyristoyl-*sn*-glycero-3-phosphatidylcholine (DMPC); 1,4-dithio-DL-threitol (DTT); dimethylformamide (DMF); 4-morpholinepropanesulfonate (MOPS); and tris(hydroxymethyl)aminomethane (Tris) were obtained from Sigma. Ethylenediaminetetraacetic acid (EDTA), glutathione (reduced), and sodium dodecyl sulfate (SDS) were from Fluka. Sephadex G-25 (fine) was from Pharmacia, and 5-(iodoacetamido)fluorescein (IAF) was from Molecular Probes.

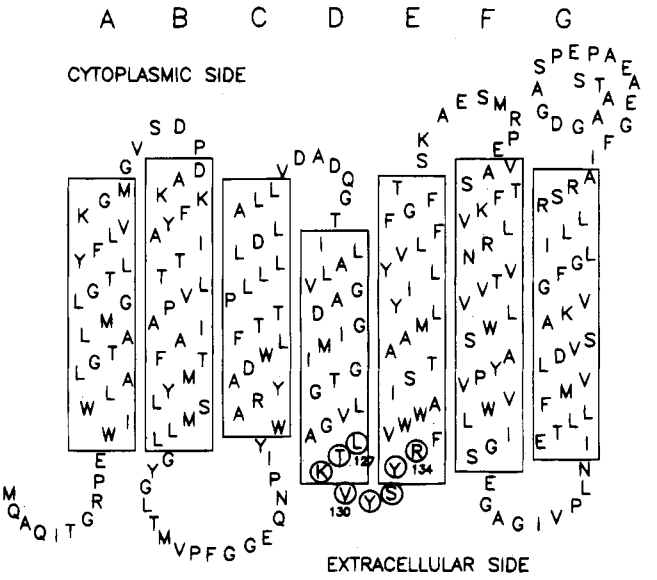

FIGURE 1: Secondary structural model of bacteriorhodopsin. The residues changed to cysteine and derivatized with fluorescein are circled.

Bacterioopsin Mutants. The construction of genes coding for mutants containing single cysteine residues at positions 125−142, their expression in *Escherichia coli*, and the purification of the bacterioopsin apoproteins have all been described (Altenbach et al., 1990; Marti et al., 1991).

Folding, renaturation of bacterioopsin, and labeling with (iodoacetamido)fluorescein are described in the preceding paper (Scherrer et al., 1994). The labeling stoichiometry, molecule of fluorescein per molecule of bR, was determined spectroscopically using an extinction coefficient of ϵ = 68 000 M^{-1} cm^{-1} (Molecular Probes) for the alkaline form of fluorescein at 495 nm and of ϵ = 52 000 M^{-1} cm^{-1} for bR at 550 nm (London & Khorana, 1982).

Flash spectroscopy was performed as described elsewhere (Otto et al., 1989). The excitation was with 10-ns pulses of 3-6 mJ of energy at 590 nm.

Flash-induced proton release and uptake were detected in the aqueous bulk medium of the micellular suspension (containing 4−10 μM bR in 0.1% CHAPS, 0.0025% DMPC, and 150 mM KCl) by measuring the difference of the flash-induced absorbance change at 450 nm between samples with and without 45 μM pyranine at pH 7.3 and 22 °C (DIFPY). For the light-induced proton concentration change with fluorescein attached to cysteine residues in bR, the flash-induced absorbance difference was determined at 495 nm between samples with and without 10 mM MOPS buffer at pH 7.3 and 22 °C (DIFAF). The buffer had no effect on the photocycle kinetics.

RESULTS

Attachment of Fluorescein to Cysteine Residues in bR. The isolated bO mutant proteins containing a single cysteine residue in the selected positions were folded and regenerated to form micelles prior to the reaction with (iodoacetamido)-fluorescein. The reaction conditions were initially worked out for bR micelles with a cysteine in position 72 of the BC loop (Scherrer et al., 1992, 1994; Alexiev et al., 1994). This reaction procedure was used successfully with cysteine on the extracellular side in the eight consecutive positions 127−134 (Figure 1). The incorporation of fluorescein was 0.7−1 mol of AF/mol of bR, except for position 127 where a

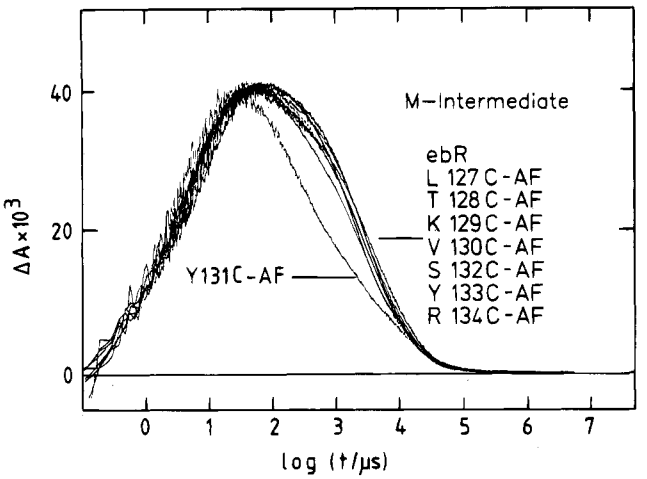

FIGURE 2: Flash-induced absorbance changes at 410 nm for ebR and the cysteine mutants in position 127−137 with fluorescein attached.

stoichiometry of only 0.25 was achieved. The mutant proteins with cysteine in the adjacent internal positions 125, 126 (helix D), and 135−142 (helix E) could not be labeled, presumably due to the lack of accessibility of their sulfhydryl groups to the bulky fluorescein.

Photocycle Kinetics and Flash-Induced Proton Concentration Changes. Most of the bR mutants showed the same absorbance spectrum and photocycle kinetics like wild type (ebR). Only in the mutants Y131C and R134C did we detect changes in the absorbance spectrum (shoulder at 500 nm) and in the photocycle kinetics within 1−2 weeks of regeneration. These changes were reversible after the addition of dithiothreitol, a reducing agent, and were thus due to oxidation of the sulfhydryl group. For the mutant L127C, a small blue shift (approximately 6 nm) in the absorbance maximum was observed. The labeled mutant bRs showed the same photocycle kinetics as seen for the unlabeled, except for Y131C-AF which had minor changes in the M decay (Figure 2). The time range in which the proton is released is roughly concurrent with the formation of the M-intermediate, which is the same for all labeled mutants and ebR (Figure 2 and Table 1). This allowed a meaningful comparison of the proton release times in the various positions.

The proton release kinetics were obtained from the difference of the absorbance changes at 495 nm between buffered and unbuffered labeled samples. By using this difference, possible effects on the pK_{app} of fluorescein by transient surface potental changes could be excluded (Alexiev et al., 1994). The time course of the photocycle at 650 and 410 nm as well as the kinetics of proton release and uptake, detected by fluorescein bound to the protein and by pyranine in the aqueous bulk phase, were measured in 150 mM KCl at pH 7.3 and 22 °C. The kinetic data for ebR and the mutants are summarized in Tables 1 and 2. For all mutants and ebR, the rise of M (Table 1) has a fast component around 1 μs with approximately 30% of the amplitude and a 10 times slower component around 10 μs with 60% of the amplitude. This clear temporal separation into two major components of comparable amplitude should facilitate the assignment of the proton release time to either one of these components if a kinetic correlation exists.

Table 1: Kinetics of M Formation and Proton Release Detected in Positions of Helices D and E and in Connecting Loop[a]

label position	M intermediate rise (μs)		H^+ release	
			DIFAF (μs)	DIFPY (μs)
ebR	0.9(33)	9.3(58)	69	126
L127C-AF	1.6(33)	9.1(60)	10	130
T128C-AF	1.4(30)	14.0(60)	69	110
K129C-AF	0.8(30)	9.1(60)	60	114
V130C-AF	1.5(31)	11.5(60)	22	136
Y131C-AF	1.4(41)	8.9(49)	33	130
S132C-AF	1.4(30)	12.3(65)	26	120
Y133C-AF	1.2(30)	9.0(60)	76	130
R134C-AF	1.0(30)	7.0(60)	27	130

[a] The M formation is measured as the absorbance increase at 410 nm in 150 mM KCl, pH 7.3, at 22 °C. The relative contributions of the two main components in the formation of M are given as percentages in parentheses following the rise times. The proton release is detected with fluorescein bound to the position indicated at 495 nm (DIFAF) and with pyranine in the aqueous bulk phase at 450 nm (DIFPY). In the case of ebR, proton release with fluorescein was measured with CAF adsorbed to the micelle.

Table 2: Kinetics of M Decay and Proton Uptake[a]

label position	M intermediate decay (ms)			H^+ uptake	
				DIFAF (ms)	DIFPY (ms)
ebR	0.4(15)	1.8(50)	9.8(31)	4.3/13.1	3.8/13.8
L127C-AF	0.3(18)	2.5(48)	12.6(28)	12.4	3.2/22.0
T128C-AF	1.0(22)	2.2(50)	13.8(28)	8.2	1.7/14.4
K129C-AF	1.7(25)	2.6(35)	11.5(35)	9.1	3.2/14.1
V130C-AF	0.4(20)	2.3(50)	14.3(25)	9.1	3.5/14.0
Y131C-AF	0.2(28)	1.2(29)	7.6(24)	8.0	3.0/20.0
S132C-AF	0.4(17)	1.9(50)	13.0(30)	10.1	2.1/10.7
Y133C-AF	0.6(18)	2.4(50)	11.6(30)	8.1	1.9/6.6
R134C-AF	0.3(20)	1.3(50)	8.1(30)	10.0	3.0/10.8

[a] The conditions are as given in Table 1. The relative contributions of the main components in the decay of M are given as percentages in parentheses following the decay times. When two components occur in the proton uptake, the times are separated by a slash.

Proton Release Times Vary with Indicator Attachment Site. In the preceding paper, proton release times of approximately 20 μs were obtained with fluorescein in positions 72 and 130 on the extracellular surface. For fluorescein in positions 127−134, similar proton release times might have been expected. Surprisingly, only the indicator at positions 127, 131, 132, and 134 displayed proton release times of 10−30 μs, whereas the indicator at positions 128, 129, and 133 showed release times of 60−80 μs (Table 1). The slower release times were about the same as those observed with fluorescein bound on the cytoplasmic side (61 ± 4 μs) and with CAF adsorbed to ebR micelles (69 μs) (Scherrer et al., 1994). In other words, roughly two classes of fluorescein positions could be distinguished on the extracellular side. The proton release times obtained in the region of the DE-loop are plotted versus the label position in Figure 3. There are three consecutive label positions (130, 131, 132) with a fast release time, whereas the dye in the adjacent positions detected the proton with a 2−3-fold delay. The proton release kinetics to the bulk medium detected with pyranine were similar for all these mutants and ebR (110−136 μs). As an example of the fast and slow proton release times in neighboring positions, Figure 4 shows the kinetics of the proton signal (450 nm for pyranine; 495 nm for fluorescein) and the M-intermediate (at 410 nm) for K129C-AF and

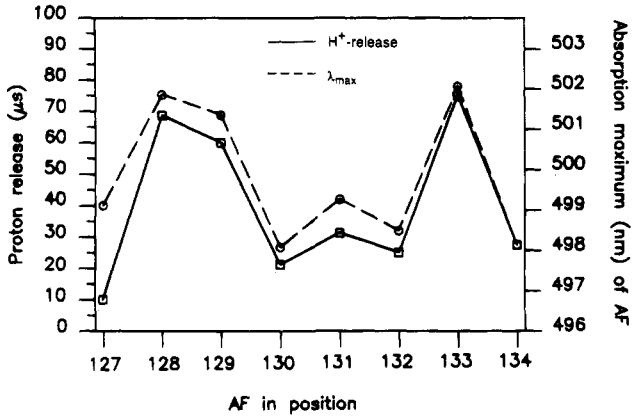

FIGURE 3: Plot of the proton release time and the absorbance maximum of fluorescein as a function of the label position. The samples were in 0.1% CHAPS, 0.0025% DMPC, and 150 mM KCl, pH 7.3, at 22 °C.

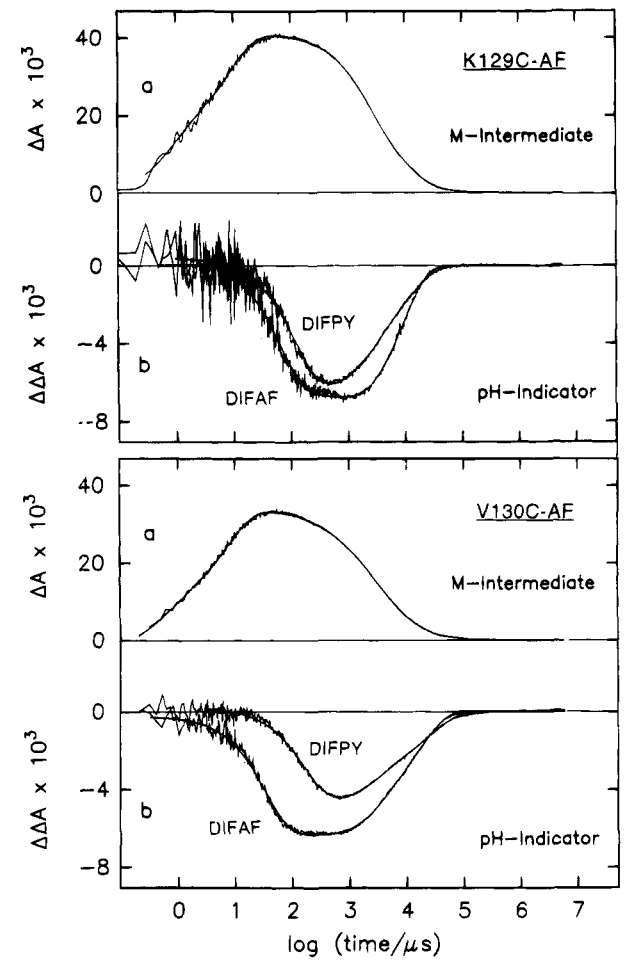

FIGURE 4: Comparison of the rise and decay of the M intermediate at 410 nm (a) with the kinetics of the proton release and uptake (b) for K129C-AF and V130C-AF. In panel b, the proton signal as detected by bound fluorescein at 495 nm is the absorbance difference between unbuffered and buffered (10 mM MOPS) samples (DIFAF). The proton signal in the bulk as sensed by pyranine at 450 nm is the absorption difference between samples with and without pyranine (DIFPY). A negative $\Delta\Delta A$ indicates the release of protons. The solid lines represent multiexponential fits. The samples were in 0.1% CHAPS, 0.0025% DMPC, and 150 mM KCl, pH 7.3, at 22 °C. The excitation was at 590 nm with 10-ns flashes of 3−6 mJ. The logarithmic time scale is from 1 to 10^7 μs.

V130C-AF. The release time obtained in position 129 of 60 μs is clearly slower than that for position 130 of 22 μs.

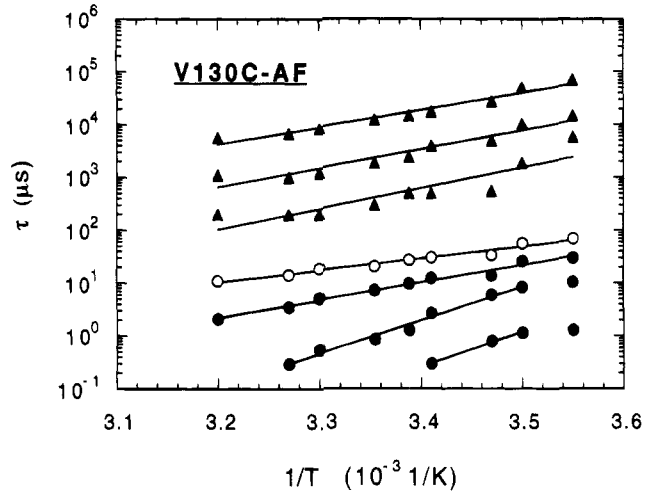

FIGURE 5: Arrhenius plot of the time constants for formation (●) and decay (▲) of the M-intermediate and for the proton release (○) measured with fluorescein bound to position 130 (V130C-AF). The samples were in 0.1% CHAPS, 0.0025% DMPC, and 150 mM KCl at pH 7.3.

Polarity of Label Environment Varies with Attachment Site. This distinct difference in the detection time for the released proton in positions within the same extracellular loop region could be the result of different orientations for the label molecules into environments of possibly distinct polarity. This may be accompanied by environmental effects on the absorption maximum of the bound dye. The absorption maximum of fluorescein is dependent on the polarity of the solvent and shifts to higher wavelength when the solvent becomes more apolar. This was tested with CAF in water and in ethanol/water mixtures. The absorption maximum of fluorescein in the aqueous solution was at 490 nm, whereas in an ethanol/water mixture with a dielectric constant of 25 it was shifted to 498 nm. A dependency of the dye absorption maximum on the label position could thus provide information on the polarity of its environment. In Figure 3, the absorption maxima determined for the bound fluorescein are plotted versus the label position. A dependency of the absorption maximum on the label position is apparent. The correlation with the proton release times is excellent, in particular if we consider the error of ±0.5 nm in the absorption maximum and ±4 μs in the release times.

Comparison of Kinetics of M Formation and Proton Release. Table 1 allows a comparison between the kinetics of M formation and of proton release. It is apparent that the proton release as detected with a surface-bound dye is always delayed with respect to the slowest component in the rise of M except for position 127. With fluorescein in this position, two components were observed in the proton release kinetics. The fast component of approximately 10 μs (25−50% of the signal amplitude) agrees well with that of the slowest component in the rise of the M intermediate.

Temperature Dependence of Proton Release and M Formation. The kinetics of the M-intermediate and the proton release were measured in the temperature range 5−40 °C with fluorescein in position 128 and 130 with a slow and fast release time, respectively. The Arrhenius plots of the proton release time and of the rise and decay times of the M-intermediate are shown in Figure 5 for the mutant V130C-AF. The straight lines represent least squares fits of the data points. Note that in Figure 5 there are three

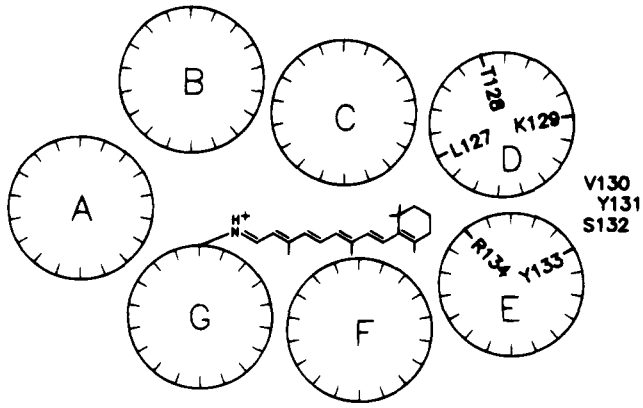

FIGURE 6: Helical wheel plot of bR with the orientation for helices D and E as proposed, based on the data in Figure 3.

components shown for the rise of M at temperatures below 20 °C. The kinetic constants in Table 1 refer to the data at 22 °C. At this temperature, the two slowest rise components make up 90−95% of the amplitude. For V130C-AF, the two fastest exponentials of the M rise have the same activation energy of about 115 kJ/mol. The activation energy of the slowest component in the M rise which contributes 60% to the absorbance increase is 65 ± 5 kJ/mol and coincides approximately with that of the proton release time (52 ± 5 kJ/mol). At position 72 in the BC loop, like 130 a position with a fast proton release time (21 μs), a similar activation energy for the proton release of 54 kJ/mol was determined (data not shown). In position 128 on the other hand, with a slow proton release time of 69 μs, the activation energy was only 25 kJ/mol (data not shown). On the cytoplasmic side with fluorescein attached to position 35 [proton release of 61 μs (Scherrer et al., 1994)], a low activation energy similar to the one in position 128 was obtained for the proton release (data not shown).

DISCUSSION

In the preceding paper, we determined the proton release time on the extracellular side with the pH-indicator fluorescein attached to positions 72 (BC loop) and 130 (DE loop) and in the loops on the cytoplasmic side. In this study, we labeled eight successive positions (127−134) in the DE loop and the amino acids preceding and following this loop. We obtained two distinctly different groups of release times with the bound fluorescein: either 10−30 μs or about 70 μs, suggesting two discrete environments for the fluorescein probe. Since the photocycle kinetics are unchanged and the release time detected with pyranine in the aqueous bulk medium is the same in all these samples, the differences in the proton release time must be ascribed to the specific positioning and orientations of the probe at these successive sites. Indeed, the differences observed give us confidence that we are able to detect the arrival of the proton at the protein surface immediately after their release.

The pattern of slower and faster release times as a function of the label position shown in Figure 3 may be explained with reference to the helical wheel model shown in Figure 6. The three sites, 130−132, where fast release kinetics were obtained are residues in the loop between helix D and helix E. In these positions, the label has enough freedom to rotate or to orient itself on the protein surface permitting an early detection of the pumped proton. Residues 127−129 are part of helix D with 127 oriented toward the proton channel (fast proton detection) and 128 and 129 (slow proton detection) oriented toward the outside of the protein (Figure 6). Residue 133 is the first one in helix E oriented toward the outside with a slow release time, and 134 is the second residue in helix E oriented toward the inside with a fast time. The position and size of the short loop consisting of residues 130−132 actually agrees well with the structure for this region proposed by Altenbach et al. (1990) based on ESR studies with spin labels attached to cysteines in the same positions. A short loop between helix D and helix E was also proposed by Engelman et al. (1980) and Huang et al. (1982). These authors considered residue 130 already as part of helix D. If this is the case, then based on our proton release data, residue 130 would be oriented toward the proton channel as the last amino acid in helix D leading to approximately the same orientation for helix D as the one presented in Figure 6. The proposed large loop from residue 128 to residue 135 (Henderson et al., 1990) is not consistent with our data. The rotational orientation of helix E is in excellent agreement with both the results of high-resolution electron microscopy (Henderson et al., 1990) and the spin label studies of Altenbach et al. (1990). For helix D, on the other hand, there is no agreement with the structural model of Henderson and co-workers. However, the rotational orientation of helix D was only poorly defined in the electron density map since it contains no bulky aromatic side chains and is therefore the least certain (Henderson et al., 1990). In a recent study, the rotational orientations of the transmembrane α-helices of bacteriorhodopsin were investigated using model calculations in which the observed and calculated neutron diffraction intensities of specifically deuterated purple membranes were compared on the basis of the χ_ν^2 criterion (Samatey et al., 1994). For helix D, two distinct minima were obtained for χ_ν^2 as a function of the rotation angle around the helix axis: one for an orientation close to the one suggested by Henderson et al. (1990) and the other for an orientation similar to the one proposed here. In the folded active form, the cysteine residues in positions 125 and 126 (helix D) and in positions 135−142 (helix E) could not be labeled, presumably because they are buried inside the protein or shielded by the lipid/detergent phase. The strategy described here for determining the orientation of helices D and E could therefore not be pursued with these internal residues.

Another approach to obtain information about the orientation of helices is to investigate the effect of the polarity of the environment on the absorbance maximum of the bound label in the various positions. The absorbance maximum of fluorescein is shifted to longer wavelength when it is moved from a polar environment to an apolar environment. There is an additional small shift in the absorbance maximum to longer wavelength for the bound versus unbound fluorescein. The values for the absorbance maximum thus provide information about the polarity of the label environment. The distinct shifts observed for the eight positions studied (Figure 3) can indeed be interpreted in terms of a rather hydrophilic environment for the label in the loop positions and in positions pointing toward the interior and a more hydrophobic environment for the dye oriented toward the outside, to the detergent/lipid area. This interpretation agrees very well with the proposed orientation based on the proton release kinetics. Similarly, the absorbance maxima

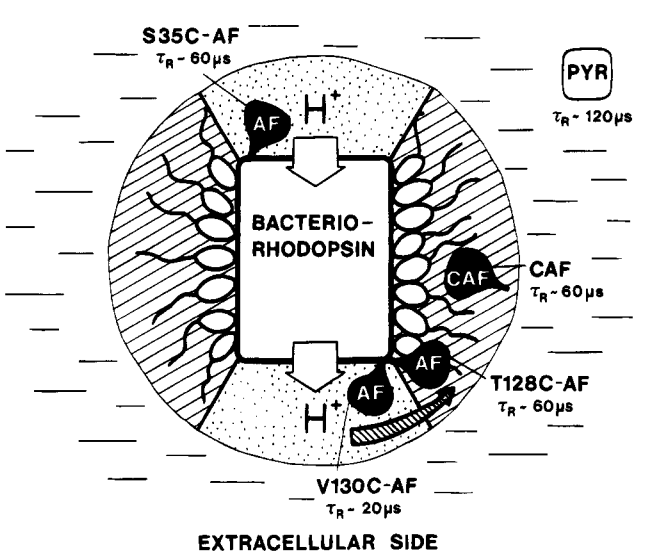

FIGURE 7: Cartoon of the bR micelle. The CHAPS molecules are drawn schematically with a hydrophobic head and a hydrophilic tail according to their chemical structure. The boundary layer protein-bulk and detergent/lipid-bulk are marked by stippling and hatching, respectively.

for the dye in the various cytoplasmic positions provide information about their environment. The values obtained indicate a hydrophilic environment (absorption maximum of about 497 nm) for all cytoplasmic positions investigated in the preceding paper (Scherrer et al., 1994).

Based on our results for proton detection times, the model in Figure 7 is proposed. Because similar proton release times are detected on the cytoplasmic side as on the extracellular side with the dye molecule oriented toward the detergent/lipid environment, the rate-limiting step for the proton to move around the bR micelle surface appears to be between the extracellular protein surface and the micelle (detergent/lipid) surface. This is supported by the results of the calculated activation energy for the proton release detected in positions 130 (DE loop) and 128 (helix D, oriented toward the micellular surface). The activation energy refers to the rate-limiting step. The activation energies for the proton release obtained for positions 130 and 128 differ by approximately 30 kJ/mol, indicating different rate-limiting steps. This is interpreted as a rate-limiting energy barrier for the proton to migrate from the protein to the micellular (detergent/lipid) boundary layer (arrow in Figure 7). The proton movement within the micellular boundary layer would thus be faster than a few microseconds, since the slow release times observed on the extracellular side are similar to the release times determined on the cytoplasmic side (Scherrer et al., 1994).

The activation energy calculated for position 130 (52 ± 5 kJ/mol) agrees well with that calculated for the slowest M-rise component (65 ± 5 kJ/mol). However, the proton release time is ≈22 μs versus ≈10 μs for the slowest M-rise component at 22 °C. Thus, there is a time delay of at least 10 μs between the release of the proton from the Schiff base and the time a proton is detected on the surface. Similar delays were observed for all other positions with fast release times (Y131C-AF, S132C-AF, R134C-AF). With cysteine in position 127, only 25% incorporation of fluorescein was achieved, suggesting this residue to be further inside the protein. This is supported by the reduced accessibility of fluorescein in this position for externally added protons as measured by the abnormally low value of the dye absorbance change per proton added. The number obtained is 4-fold lower than that for the other labeling sites. In this position, we detected the fastest proton release time of about 10 μs. In L127C-AF, the slowest rise time of M, which is also the major component (about 60%), and the proton release time coincide. This places the fluorescein in position 127 in the direct path of the proton. The delay of about 10 μs between proton detection and the slowest component in the rise of M observed at the other positions may represent the equilibration step within the extracellular protein boundary layer.

We conclude that kinetically the proton release is coupled with the slowest component in the rise of M, at least at position 127. One advantage of the micelle system over purple membranes is that the rise of M is separated in time in two components of comparable amplitudes with rise times which differ by a factor of 10. This allows an unambiguous assignment of proton release to either one of these components. We can conclude that there is no proton release associated with the faster rising component but that a likely correlation exists with the slowest component. There are currently several alternative kinetic interpretations of the slowest rise time of M. With one M species, the multiple rise times may be interpreted by invoking back-reactions. Another possibility is that there are parallel photocycles, each with its own M rise time. Recently, evidence has been presented for the existence of at least two sequential M substates in purple membranes and bR micelles. With bR in Triton X-100 micelles, a marked wavelength shift occurred between early and late M, and two sequential substates M_1 and M_2, well separated in time and of comparable amplitude, were observed (Váró & Lanyi, 1991; Váró et al., 1992). The latter is quite similar to our observations with bR/CHAPS/DMPC micelles. From the pH dependence of the rate constants, it was also suggested that proton release does not occur between L and M but between these two M states (Zimányi et al., 1992). Thus, without a further detailed analysis of the photocycle kinetics, we cannot distinguish between the alternatives of proton release being coupled to the second component of the L to M transition (as a consequence of back-reaction) or to the transition between two M states.

The characterization of the various label positions in terms of light-induced proton release now permits the selection of appropriate label positions to answer specific questions in regard to mutants with impaired or altered photocycle and proton release. For example, the mutant R82A has an accelerated M rise but a reversed order of proton release and uptake. The latter conclusion was based on data obtained with pyranine in the aqueous bulk phase (Otto et al., 1990). R82A/cysteine double mutants will allow the attachment of fluorescein on the extracellular side, permitting an accurate determination of the proton release time.

REFERENCES

Alexiev, U., Marti, T., Heyn, M. P., Khorana, H. G., & Scherrer, P. (1994) *Biochemistry, 33*, 298−306.

Altenbach, C., Marti, T., Khorana, H. G., & Hubbell, W. L. (1990) *Science 248*, 1088−1092.

Bousché, O., Sonar, S., Krebs, M. P., Khorana, H. G., & Rothschild, K. J. (1992) *Photochem. Photobiol. 56*, 1085–1095.

Braiman, M. S., Mogi, T., Marti, T., Stern, L. J., Khorana, H. G., & Rothschild, K. J. (1988) *Biochemistry 27*, 8516–8520.

Ebrey, T. G. (1993) in *Thermodynamics of Membrane Receptors and Channels* (Jackson, M. B., Ed.) pp 353–387, CRC Press, Boca Raton, FL.

Engelman, D. M., Henderson, R., McLachlan, A. D., & Wallace, B. A. (1980) *Proc. Natl. Acad. Sci. U.S.A. 77*, 2023–2027.

Henderson, R., Baldwin, J. M., Ceska, T. A., Zemlin, F., Beckmann, E., & Downing, K. H. (1990) *J. Mol. Biol. 213*, 899–929.

Huang, K.-S., Radhakrishnan, R., Bayley, H., & Khorana, H. G. (1982) *J. Biol. Chem. 257*, 13616–13623.

London, E., & Khorana, H. G. (1982) *J. Biol. Chem. 257*, 7003–7011.

Lozier, R. H., Niederberger, W., Bogomolni, R. A., Hwang, S. B., & Stoeckenius, W. (1976) *Biochim. Biophys. Acta 440*, 545–556.

Marti, T., Rösselet, S. J., Otto, H., Heyn, M. P., & Khorana, H. G. (1991) *J. Biol. Chem. 266*, 18674–18683.

Mathies, R. A., Lin, S. W., Ames, J. B., & Pollard, W. T. (1991) *Annu. Rev. Biophys. Chem. 20*, 491–518.

Oesterhelt, D., & Stoeckenius, W. (1973) *Proc. Natl. Acad. Sci. U.S.A. 86*, 9228–9232.

Otto, H., Marti, T., Holz, M., Mogi, T., Lindau, M., Khorana, H. G., & Heyn, M. P. (1989) *Proc. Natl. Acad. Sci. U.S.A. 86*, 9228–9232.

Otto, H., Marti, T., Holz, M., Mogi, T., Stern, L. J., Engel, F., Khorana, H. G., & Heyn, M. P. (1990) *Proc. Natl. Acad. Sci. U.S.A. 87*, 1018–1022.

Racker, E., & Stoeckenius, W. (1974) *J. Biol. Chem. 249*, 662–663.

Samatey, F. A., Zaccaï, G., Engelman, D. M., Etchebest, C., & Popot, J.-L. (1994) *J. Mol. Biol. 236*, 1093–1104.

Scherrer, P., Alexiev, U., Otto, H., Heyn, M. P., Marti, T., & Khorana, H. G. (1992) in *Structures and Functions of Retinal Proteins* (Rigaud, J. L., Ed.) Vol. 221, pp 205–211, Colloque INSERM, John Libbey Eurotext Ltd., Montrouge, France.

Scherrer, P., Alexiev, U., Marti, T., Khorana, H. G., & Heyn, M. P. (1994) *Biochemistry 33*, 13684–13692.

Stoeckenius, W., & Bogomolni, R. A. (1982) *Annu. Rev. Biochem. 52*, 587–615.

Tittor, J., Soell, Ch., Oesterhelt, D., Butt, H.-J., & Bamberg, E. (1989) *EMBO J. 8*, 3477–3482.

Váró, G., & Lanyi, J. K. (1991) *Biochemistry 30*, 5008–5015.

Váró, G., Zimányi, L., Chang, M., Ni, B., Needleman, R., & Lanyi, J. K. (1992) *Biophys. J. 61*, 820–826.

Zimányi, L., Váró, G., Chang, M., Ni, B., Needleman, R., & Lanyi, J. K. (1992) *Biochemistry 31*, 8535–8543.